On-line parameter estimation of a magnetic bearing

Romain Delpoux, Thierry Floquet

On-line parameter estimation of a magnetic bearing

Romain Delpoux and Thierry Floquet

***Abstract*— This article presents a parameter estimation algorithm for a magnetic bearing. Such process are inherently unstable systems with strongly nonlinear dynamics. Here, a simplified model of the magnetic bearing is developed in order to be able to estimate certain parameters. These parameters are measurable with difficulty, and may slightly vary over time. The expression of the estimates is written as a function of integrals of the inputs and outputs of the system. The experiments show a fast and robust on-line identification.**

***Index Terms*— Parameter estimation, Laplace transform, Magnetic bearing.**

I. INTRODUCTION

Magnetic bearings can be used for machine tool spindles to produce circular and non-circular holes with high precision. They have the advantage to have a contact free suspension. Specially in high speed applications, magnetic bearings won importance. They provide advantages compared to conventionnel bearings such as no lubrification and no frictions). This improves reliability and performances. There is a real industrial demand for such process which allow non-circular motion of the order of 50 micro-meters. The required precision is really important : Path tracking error must be less than 1 micro-meter on circular paths and 3 micro-meters on non-circular ones with a rotation speed up to 1000 rpm.

The magnetic shaft used in our laboratory consists of one electromagnetic radial bearing and two axial bearings. It is similar to the one presents in [4]. It is an inherently unstable system where the dynamics are strongly nonlinear. We refer to the work [3], [4], [9], [10], [11] concerning the control of such systems.

The goal of this paper concerns the estimation of parameters of the radial bearing using an algebraic approach based on the work of Fliess and Sira-Ramirez ([6], [7]). The estimation procedure given by exact formulas, leads to a non asymptotic convergence. In this approach, it is possible to express the desired parameters as a function of integrals of the measured output and the inputs of the system. This method has already been applied for parameter estimation ([8], [16]), for abrupt change detection and delays ([1], [2], [5], [15]) as well as for numerical differentiation ([12], [14]).

The article is divided into three parts. Section II presents the radial magnetic bearing and introduces problems encountered when identifying parameters. In Section III, expressions for the on-line identification of the desired parameters are developed. Here is treated the on-line estimation of parameters depending on the geometry and the materials of the radial bearing. The last Section is devoted to simulation and experimental results.

This work was supported by Nord-Pas de Calais Regional Council and FEDER through the Contrat de Projets Etat Region (CPER) 2007-2013.

R. Delpoux and T. Floquet are with the Laboratoire d'Automatique, Génie Informatique et Signal (CNRS FRE 3303), École Centrale de Lille, 59651 Villeneuve d'Ascq cedex, France and Team Non-A, INRIA Lille-Nord Europe, France. romain.delpoux@ec-lille.fr and thierry.floquet@ec-lille.fr

II. PROBLEM STATEMENT

In this article is presented an approach to estimate parameters of the radial bearing(the axial bearing case will be considered in future work). The parameters that we are trying to estimate here depend of the geometry and the material of the bearing. The estimation of these parameters is important because such parameters are difficult to calculate and are susceptible to vary slightly over time.

The rotor is levitating using a three-phase electromagnetic radial bearing, arranged like three coupled "horseshoe magnets" around the rotor (Fig. 1). The three generated current furnish three independent control inputs. The mathematical model of the bearing is based on the assumption of a rigid body and leads to decoupled equations for forces. The dynamics equations, under simplifying assumptions, are written as follows:

$$m\ddot{Y} = F_y \quad (1)$$

$$m\ddot{Z} = F_z \quad (2)$$

where Y and Z represent the coordinates of the center of mass of the rotor in a Cartesian frame (with axes y et z) which is fixed in the space, a t a point being considered as the "center" of the device. The forces F_y et F_z represent the resulting forces applied in directions y et z respectively. The rotor has a mass m. The resultante forces in the plan $(y-z)$ are given by the superposition of the forces generated by the

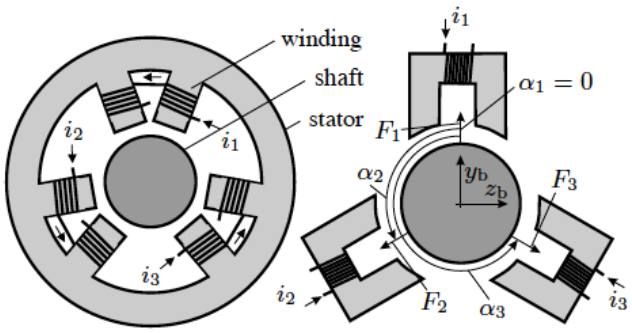

Fig. 1. Sketch of the three-phase radial bearing

magnets:

$$\begin{pmatrix} F_y \\ F_z \end{pmatrix} = \begin{pmatrix} \sin\alpha_1 & \sin\alpha_2 & \sin\alpha_3 \\ \cos\alpha_1 & \cos\alpha_2 & \cos\alpha_3 \end{pmatrix} \begin{pmatrix} F_1 \\ F_2 \\ F_3 \end{pmatrix} \quad (3)$$

The angles that appears in (3) are presented Fig. 1. Individually, the magnetic forces can be modeled by ($k \in \{1,2,3\}$):

$$F_k = \lambda_k \frac{i_k^2}{\left(s - \begin{pmatrix} \sin\alpha_k \\ \cos\alpha_k \end{pmatrix}^T \begin{pmatrix} Y_b \\ Z_b \end{pmatrix}\right)^2} \quad (4)$$

where Y_b and Z_b are the positions in the bearing plan. s is the nominal air gap and λ_k are parameters depending on the geometry and the materials of the bearing. They will be estimated on-line.

Calculating control currents: The reference currents are obtained from the desired forces. In order to simplify the notations, we assume that the bearing is symmetric, i.e. $\alpha_1 = \pi$, $\alpha_2 = -\frac{\pi}{3}$ and $\alpha_3 = \frac{\pi}{3}$. In each of the models detailed above, we obtain a couple of independent forces for each bearing plan. Choosing F_1 gives :

$$F_1 = \begin{cases} F_0 & \text{if} \quad F_z \geq \frac{|F_y|}{\sqrt{3}} \\ F_0 - \frac{|F_y|}{\sqrt{3}} + F_z & \text{else} \end{cases} \quad (5)$$

With $F_0 \geq 0$ arbitrary chosen, the two remaining forces are obtained from the model (3):

$$F_2 = F_1 + \frac{F_y}{\sqrt{3}} + F_z$$
$$F_3 = F_1 - \frac{F_y}{\sqrt{3}} + F_z$$

Then the currents are calculated from the desired magnetic forces using relation (4).

The above equations reflect the dynamics of the unperturbed model. Model simplifications in (1)-(2) and modeling errors (e.g. due to incorrect relationship between the input currents i_* and the corresponding forces F_*) are assumed to have the same effect than perturbations.

The rotor rotation is also a perturbation source with harmonic components. When the rotor moves along an ellipsoid trajectory, the positions in the directions y et z are sinusoidal function. A significant error in the relation between the currents and the forces can also change sinusoidally.

Therefore, the perturbations must be rejected in the λ_i estimation algorithm (or must be estimated in order to be compensated in the control).

The perturbed model can be written as:

$$m\ddot{Y} = F_y + p_y(t) \quad (6)$$
$$m\ddot{Z} = F_z + p_z(t) \quad (7)$$

where $p_*(t)$ represent the perturbations on each axis. Using equation (6), (7), (3) and (4), we obtain a relationship of the form:

$$\ddot{Y} = \sum_{k=1}^{3} \lambda_k u_{y,k} + \frac{p_y(t)}{m} \quad (8)$$

$$\ddot{Z} = \sum_{k=1}^{3} \lambda_k u_{z,k} + \frac{p_z(t)}{m} \quad (9)$$

with $u_{y,k} = \frac{\sin(\alpha_k) i_k^2}{m\left(s - \begin{pmatrix} \sin\alpha_k \\ \cos\alpha_k \end{pmatrix}^T \begin{pmatrix} Y_b \\ Z_b \end{pmatrix}\right)^2}$

and $u_{z,k} = \frac{\cos(\alpha_k) i_k^2}{m\left(s - \begin{pmatrix} \sin\alpha_k \\ \cos\alpha_k \end{pmatrix}^T \begin{pmatrix} Y_b \\ Z_b \end{pmatrix}\right)^2}$

These two equations depend on the measured inputs and the accelerations in the plan. The parameters λ_k are the parameters to be estimated from measurements of Y et Z and despite the perturbations. They may be difficult to compute. The identification of magnetic bearings is usually slow to be implemented and is often made off-line. In the next Section, we will develop expressions for the identification leading to an on-line, fast and robust estimation of these parameters.

III. Algebraic Approach

A. Estimation of λ_k parameters

It will be shown in this Section, that the three parameters λ_1, λ_2 and λ_3 can be estimated using equation (9). Indeed, using algebraic approach for this system, we are able to express the parameters λ_k as a function of the measured outputs and the inputs only. In order to simplify the computations, it is assumed that the perturbations are constant. We will see in the next paragraph how to deal with non constant perturbations.

Consider the Laplace transform of (9) :

$$s^2 Z(s) - sZ(0) - \dot{Z}(0) = \lambda_1 U_{Z,1}(s) + \lambda_2 U_{Z,2}(s) + \lambda_3 U_{Z,3}(s) + \frac{a}{s} \quad (10)$$

and multiply (10) by s:

$$\begin{aligned} &s^3 Z(s) - s^2 Z(0) - s\dot{Z}(0) = \\ &\lambda_1 s U_{Z,1}(s) + \lambda_2 s U_{Z,2}(s) + \lambda_3 s U_{Z,3}(s) + a \end{aligned} \quad (11)$$

Derive with respect to s trice to cancel the initial conditions and the perturbations.

$$\begin{aligned} &6Z(s) + 18s\tfrac{d}{ds}(Z(s)) + 9s^2\tfrac{d^2}{ds^2}(Z(s)) + s^3\tfrac{d^3}{ds^3}(Z(s)) \\ &= \lambda_1 \left(3\tfrac{d^2}{ds^2}(U_{Z,1}(s)) + s\tfrac{d^3}{ds^3}(U_{Z,1}(s))\right) \\ &+\lambda_2 \left(3\tfrac{d^2}{ds^2}(U_{Z,2}(s)) + s\tfrac{d^3}{ds^3}(U_{Z,2}(s))\right) \\ &+\lambda_3 \left(3\tfrac{d^2}{ds^2}(U_{Z,3}(s)) + s\tfrac{d^3}{ds^3}(U_{Z,3}(s))\right) \end{aligned} \quad (12)$$

We remind that the differentiation with respect to s in the operational domain results to a multiplication by $-t$ in the time domain. The multiplication by s in the operational domain leads to the derivation in the time domain. The application of the linear estimator (12) is then not convenient. Derivation amplify the high frequency and then the noise contribution. A simple solution is to make the estimator proper. We simply divide (12) by s^4 in order to cancel

the derivation terms and obtain a relationship with integral operators:

$$\begin{array}{l} 6s^{-4}Z(s) + 18s^{-3}\frac{d}{ds}(Z(s)) + 9s^{-2}\frac{d^2}{ds^2}(Z(s)) + s^{-1}\frac{d^3}{ds^3}(Z(s)) \\ = \lambda_1\left(3s^{-4}\frac{d^2}{ds^2}(U_{Z,1}(s)) + s^{-3}\frac{d^3}{ds^3}(U_{Z,1}(s))\right) \\ +\lambda_2\left(3s^{-4}\frac{d^2}{ds^2}(U_{Z,2}(s)) + s^{-3}\frac{d^3}{ds^3}(U_{Z,2}(s))\right) \\ +\lambda_3\left(3s^{-4}\frac{d^2}{ds^2}(U_{Z,3}(s)) + s^{-3}\frac{d^3}{ds^3}(U_{Z,3}(s))\right) \end{array} \tag{13}$$

To return to the time domain, compute the inverse Laplace transform and apply the following formula:

$$\int_0^t\int_0^{t_{k-1}}\ldots\int_0^{t_1} x(\tau)d\tau dt_1\ldots dt_{k-1} = \frac{1}{(k-1)!}\int_0^t (t-\tau)^{k-1}x(\tau)d\tau \tag{14}$$

One gets:

$$\begin{array}{rl} & \int_0^t \left[\frac{6}{3!}(t-\tau)^3 - \frac{18}{2}(t-\tau)^2\tau + 9(t-\tau)\tau^2 - \tau^3\right] Z(\tau)d\tau \\ = & \lambda_1\left(\int_0^t \left[\frac{3}{3!}(t-\tau)^3\tau^2 - \frac{1}{2}(t-\tau)^2\tau^3\right] u_{Z,1}(\tau)d\tau\right) \\ + & \lambda_2\left(\int_0^t \left[\frac{3}{3!}(t-\tau)^3\tau^2 - \frac{1}{2}(t-\tau)^2\tau^3\right] u_{Z,2}(\tau)d\tau\right) \\ + & \lambda_3\left(\int_0^t \left[\frac{3}{3!}(t-\tau)^3\tau^2 - \frac{1}{2}(t-\tau)^2\tau^3\right] u_{Z,3}(\tau)d\tau\right) \end{array} \tag{15}$$

The previous equation depends on the integrals of the measured outputs and inputs. However, there is three unknown parameters for one equation. Then, we have to generate two more equations in order to have the same number of equations than unknowns. To obtain a second equation, take equation (11) but differentiate it four times with respect to s and apply the same manipulations as before. We obtain:

$$\begin{array}{l} \int_0^t \left[-\frac{24}{3!}(t-\tau)^3\tau + \frac{36}{2}(t-\tau)^2\tau^2 - 12(t-\tau)\tau^3 + \tau^4\right] Z(\tau)d\tau \\ = \lambda_1\left(\int_0^t \left[\frac{4}{3!}(t-\tau)^3\tau^3 - \frac{1}{2}(t-\tau)^2\tau^4\right] u_{Z,1}(\tau)d\tau\right) \\ +\lambda_2\left(\int_0^t \left[\frac{4}{3!}(t-\tau)^3\tau^3 - \frac{1}{2}(t-\tau)^2\tau^4\right] u_{Z,2}(\tau)d\tau\right) \\ +\lambda_3\left(\int_0^t \left[\frac{4}{3!}(t-\tau)^3\tau^3 - \frac{1}{2}(t-\tau)^2\tau^4\right] u_{Z,3}(\tau)d\tau\right) \end{array} \tag{16}$$

The last equation is obtained, from equation (11) but differentiated it five times with respect to s. One gets:

$$\begin{array}{l} \int_0^t \left[\frac{60}{3!}(t-\tau)^3\tau^2 - \frac{60}{2}(t-\tau)^2\tau^3 + 15(t-\tau)\tau^4 - \tau^5\right] Z(\tau)d\tau \\ = \lambda_1\left(\int_0^t \left[\frac{5}{3!}(t-\tau)^3\tau^4 - \frac{1}{2}(t-\tau)^2\tau^5\right] u_{Z,1}(\tau)d\tau\right) \\ +\lambda_2\left(\int_0^t \left[\frac{5}{3!}(t-\tau)^3\tau^4 - \frac{1}{2}(t-\tau)^2\tau^5\right] u_{Z,2}(\tau)d\tau\right) \\ +\lambda_3\left(\int_0^t \left[\frac{5}{3!}(t-\tau)^3\tau^4 - \frac{1}{2}(t-\tau)^2\tau^5\right] u_{Z,3}(\tau)d\tau\right) \end{array} \tag{17}$$

Define the parameter vector: $\Lambda = \left[\begin{array}{ccc}\lambda_1 & \lambda_2 & \lambda_3\end{array}\right]^T$. Equations (15), (16) and (16) allow to obtain the expressions of the parameters $\hat{\lambda}_1$, $\hat{\lambda}_2$ et $\hat{\lambda}_3$:

$$D(t)\hat{\Lambda} = N(t) \tag{18}$$

with the matrices $D(t) \in \mathbb{R}^{3\times3}$ et $N(t) \in \mathbb{R}^{3\times1}$.
If $D(t)$ is invertible, one gets:

$$\left[\begin{array}{c}\hat{\lambda}_1 \\ \hat{\lambda}_2 \\ \hat{\lambda}_3\end{array}\right] = D(t)^{-1}N(t) \tag{19}$$

Remark 1: Note that at time $t = 0$, the matrices and vectors used to compute the estimations are null. The parameters are then undetermined. Therefore, the formula has to be calculated, not at the time $t = 0$, but at a later time, $t = \epsilon$ with $\epsilon > 0$ and small.
Thus the parameter vector is estimated as follows :

$$\hat{\Lambda} = \left\{\begin{array}{ll} \text{arbitrary for} & t \in [0, \epsilon[\\ D(t)^{-1}N(t) & t \in [\epsilon, \infty[\end{array}\right.$$

B. Implementation

In the previous paragraph, it was assumed that the perturbations were constant. Nevertheless, this is physically not realistic. It has been seen in Section II that there are two different perturbation sources.
The first perturbation source, due to simplifications and modeling error, can be consider as a constant if the signals are integrating over a small sliding window. So far, the integrals have been computed over an interval $[0, t]$ However integrating over a short time interval $[0, T_f]$ (T_f represents the window length), we can consider that the perturbations are constant. Finally we use a change of variable to reduce the estimation interval $\mathcal{I}_0^{T_f} = [0, T_f]$ to $[0, 1]$. $N(t)$ and $D(t)$ can be rewritten as:

$$N(t) = \left[\int_0^1 g_{z,i}(\tau)Z(\tau)d\tau\right]_{1\le i\le3}$$

and

$$D(t) = \left[\begin{array}{c}\int_0^1 g_{u_{z,i}}(\tau)U_{Z,j}(\tau)d\tau\end{array}\right]_{1\le i\le3,1\le j\le3}$$

with

$g_{z,1}(\tau) = \left[\frac{6}{3!}(1-\tau)^3 - \frac{18}{2}(1-\tau)^2\tau + 9(1-\tau)\tau^2 - \tau^3\right]T_f^3$
$g_{z,2}(\tau) = \left[-\frac{24}{3!}(1-\tau)^3\tau + \frac{36}{2}(1-\tau)^2\tau^2 - 12(1-\tau)\tau^3 + \tau^4\right]T_f^4$
$g_{z,3}(\tau) = \left[\frac{60}{3!}(1-\tau)^3\tau^2 - \frac{60}{2}(1-\tau)^2\tau^3 + 15(1-\tau)\tau^5 - \tau^5\right]T_f^5$
$g_{u_{z,1}}(\tau) = \left[\frac{3}{3!}(1-\tau)^3\tau^2 - \frac{1}{2}(1-\tau)^2\tau^3\right]T_f^5$
$g_{u_{z,2}}(\tau) = \left[-\frac{4}{3!}(1-\tau)^3\tau^3 + \frac{1}{2}(1-\tau)^2\tau^4\right]T_f^6$
$g_{u_{z,3}}(\tau) = \left[\frac{5}{3!}(1-\tau)^3\tau^4 - \frac{1}{2}(1-\tau)^2\tau^5\right]T_f^7$

Using the trapezoidal method, the integrals are obtained from the output of a classical FIR filter.
To reject the harmonic perturbations with frequencies close to rotational speed, the resulting numerator and denominator of each estimated parameters are filtered using a low-pass filter. The filter used is similar to the one presented in [13] :

$$\hat{\lambda}_{i,f_2}(t) = \frac{F(s)n(t)}{F(s)d(t)} \tag{20}$$

where $F(s) = \frac{\omega_n^2}{s^2+2\zeta\omega_n+\omega_n^2}$.
Experimental results are shown in the next Section.

IV. Results

We present in this section the simulation and experimental results. The numerical simulations are realized in order to show the performances of the algorithm. Finally, we will show the estimation on the real process.
The parameters are: The rotor mass is $m = 6.7(kg)$, the nominal air gap is $s = 5 \cdot e^{-4}(m)$. The control is realized as a cascade, with a current controller in the inner loop and a position controller in the outer loop. The inner loop can be characterised by a control based on the electrical model of the bearing coils. The outer is based on the rigid body

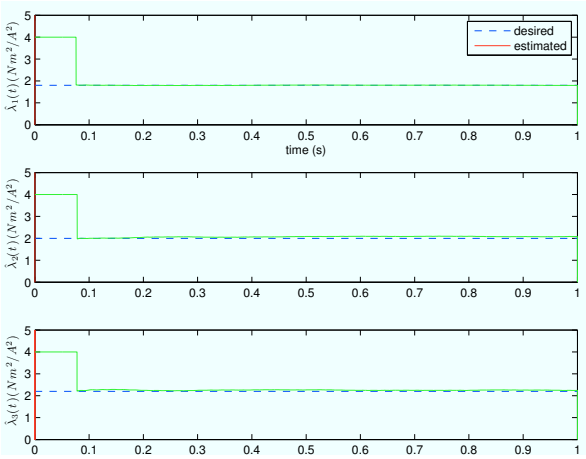

Fig. 2. Parameter estimation without noise

mechanical model. The chosen control design is a flatness based trajectory tracking control, as described in [11]. The reference trajectory is an elliptic one where $Y^* = r_Y \cos(\omega t)$ and $Z^* = r_Z \sin(\omega t)$ with $r_Y = 30.10^{-6}(m)$ and $r_Z = 70.10^{-6}(m)$. The shaft is rotating with an angular velocity of about 3000 rpm, i.e. $\omega = 50 \cdot 2\pi[rad/s]$.

The estimator is implemented in a discretized way with a sampling frequency of $1 \cdot 10^{-4}(s)$. The choice of the window length is not straightforward. The window has to be sufficiently long to cancel the noise but not too long to keep the assumption on the constant perturbation true. The experiment shows that a window $T_f = 0.02s$ gives good results. The initial value of $\lambda_{k,0}$ is set arbitrarily. The filter $F(s)$ is chosen with $\zeta = 0.707$ and $w_n = 15rad/s$.

At the beginning of the experiment, the controller uses the initial and arbitrary $\lambda_{k,0}$ from $t = 0$ to $t = t_e$, t_e being the convergence time of the algorithm. The estimator, connected in parallel to the system, estimates the parameters $\hat{\lambda}_k$ in real time on the interval $(\epsilon, t_e]$. As soon as the estimations have converged to constant values, the initial values $\lambda_{k,0}$ are replaced by the estimated values.

Fig. 4. Magnetic bearing test-bench

A. Simulation Results

In the simulations, the parameters λ_k are chosen such that $\lambda_1 = 1.8e^{-6}$, $\lambda_2 = 2e^{-6}$, $\lambda_1 = 2.2e^{-6}$. The initial value of the estimation is $\lambda_{k,0} = 4e^{-6}$. To estimate the parameters, we choose sinusodal perturbations with constant part to be similar to the real perturbations.

Fig. 2 presents the parameters estimation. On this figure, we can see that the three parameters converge to the desired value in less than 0.1 second with $\hat{\lambda}_1 = 1.786e^{-6}$, $\hat{\lambda}_2 = 2.072e^{-6}$ and $\hat{\lambda}_3 = 2.199e^{-6}$. It represents an error less that 3.5%. On the Fig. 3 we show the trajectory tracking evolution of the axe z only (the y axe is similar). In order to observe the behavior the estimated parameters are updated after 0.2 seconds. Due to the observer, before identification, the position errors are already small. However, the perturbations estimation is far from the real perturbation. It reflects the modeling errors. After parameters update, the position error is slightly decrease while the perturbation error is considerably decrease. The model is more correct, then the observed perturbation is close to the real one.

B. Experimental Results

In this Section the experimental results are presented. The test-bench is shown Fig. 4. The computer hardware on the

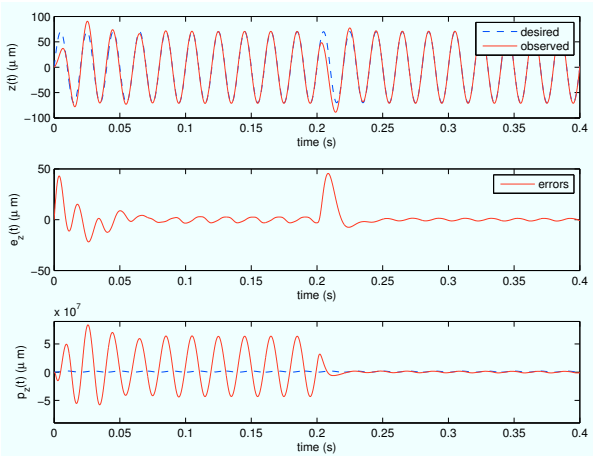

Fig. 3. Trajectory tracking evolution of z axe

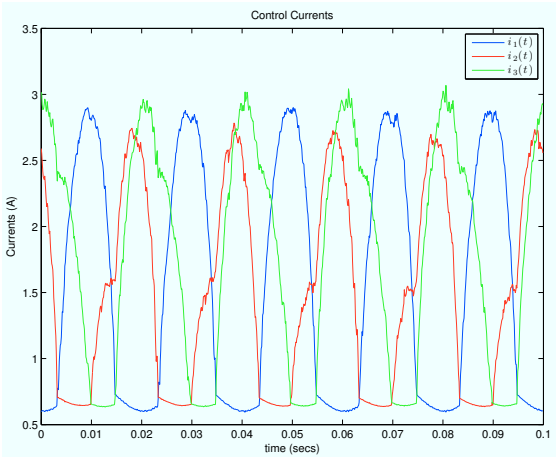

Fig. 5. Control Currents

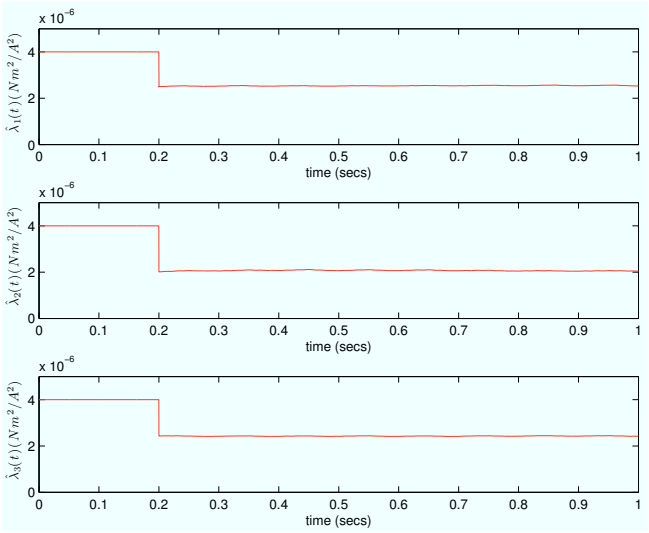

Fig. 6. Experimental estimation of the parameters

test-bench is a dSpace 1103. The control law is implemented in C and linked to the mechanical unit through Control Desk software. All currents are generated by 3 Dc brush amplifiers that serve as three independent control inputs (Fig. 5).

When the experiment starts, one does not have precise knowledge of λ_k. As in simulation, the parameters are set arbitrarily equal to $4e^{-6}(\mu m)$. The estimation algorithm starts at the beginning of the experiment. Fig. 6 shows that after 0.2 seconds, the parameters have converged. Indeed, we obtain three constant values for the parameters ($\hat{\lambda}_1 = 2.53e^{-6}$, $\hat{\lambda}_2 = 2.04e^{-6}$ and $\hat{\lambda}_1 = 2.42e^{-6}$).

In order to check estimation accuracy of the parameters, we observe the trajectories and the perturbations before and after estimation. Fig. 7 and 8 show the evolution of the y and z axes before identification while Fig. 9 and 10 show the evolution after identification. Similarly to the simulation, the most obvious result is on the perturbations. An estimate of the latter is obtained using the perturbation observer given in [11]. The amplitude of the perturbations is at least three

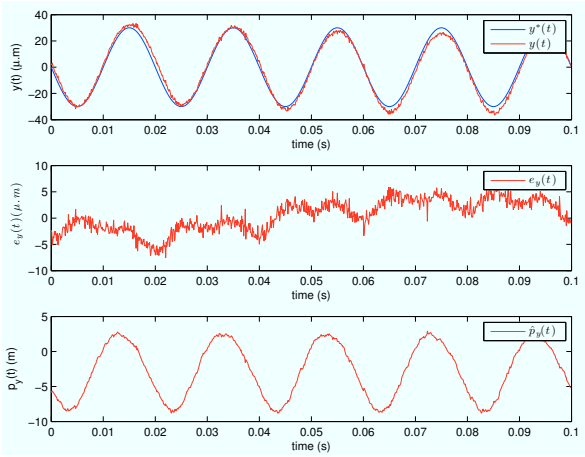

Fig. 8. Trajectory tracking evaluation on the z axe before identification

times smaller after identification than before and leads to an significant reduction of the modeling uncertainties.
Concerning the trajectories tracking and their errors, the improvement is less sensitive. Looking at the errors, we remark that the positions errors are slightly lower when the parameters are well estimated and especially more regular. The behavior is not really different, but this is not surprising. Indeed, the designed control law compensate the perturbation which is itself estimated by and observer. Estimating the perturbation, the observer takes in consideration the modelling error. Finally the last plots (Fig. 11 and 12) gives an idea of the shape of the hole before and after identification.

V. CONCLUSIONS AND FUTURE WORKS

In this article, it has been presented an estimator able to evaluate in a fast way and simultaneously several unknown parameters of a radial magnetic bearing. This system is strongly nonlinear and unstable. The performances of this algorithm show good experimental results. Indeed, the estimation is not only robust, the estimation error is low in spite of noise, but also fast, with convergence time of 0.2

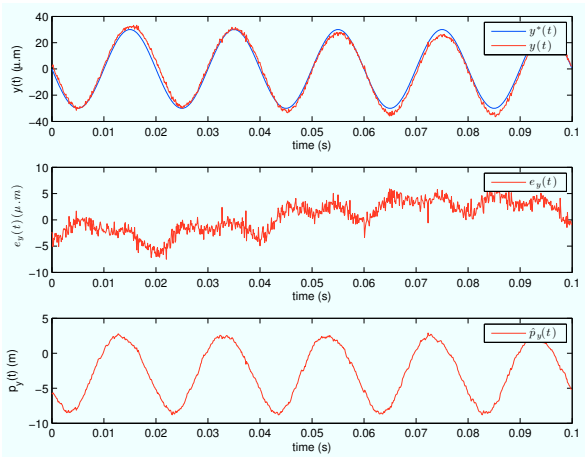

Fig. 7. Trajectory tracking evaluation on the y axe before identification

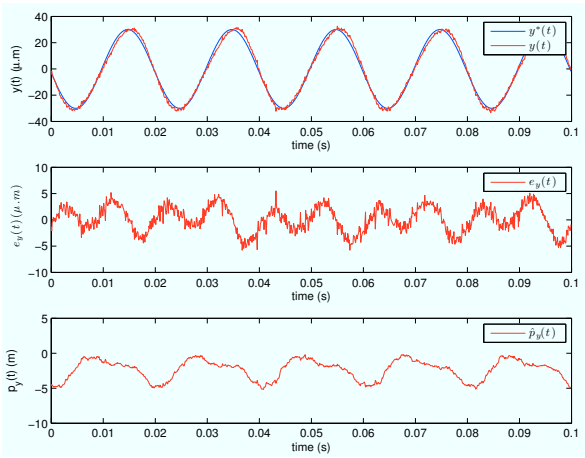

Fig. 9. Trajectory tracking evaluation on the y axe after identification

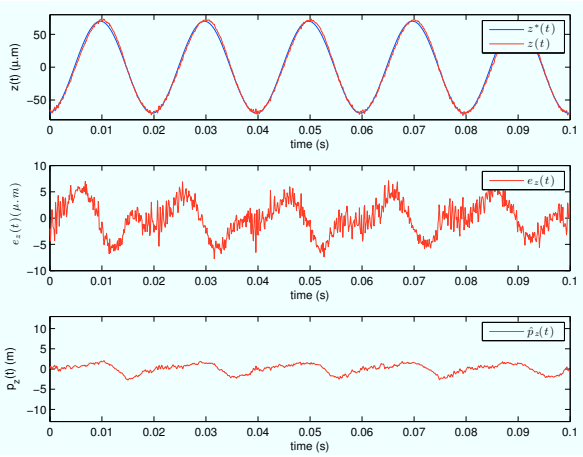

Fig. 10. Trajectory tracking evaluation on the z axe after identification

seconds. Using the estimated parameters, the trajectories are well tracked. Experiments show that the maximum tracking error is around $5\mu m$ for a non-circular hole. This could be improved using better sensors than the ones used. We have presented here the first experimental result of this kind of estimator on this process. However, we have to go further to improve this methods.

As futur work, we plan to apply this algorithm to the axial bearing. The problem is similar, but there is more parameters to be estimated at the same time. It would be interesting as well to compare this method to existing methods.

REFERENCES

[1] L. Belkoura, T. Floquet, K. Ibn Taarit, W. Perruquetti, and Y. Orlov. Estimation problems for a class of impulsive systems. *International Journal of Robust and Nonlinear Control*, sous presse.

[2] L. Belkoura, J.P. Richard, and Fliess M. Parameters estimation of systems with delayed and structured entries. *Automatica*, 45(5):1117 – 1125, 2009.

[3] Hsu C.-T. and S.-L. Chen. Nonlinear control of a 3-pole active magnetic bearing system. *Automatica*, 39(2):291–298, Feb 2003.

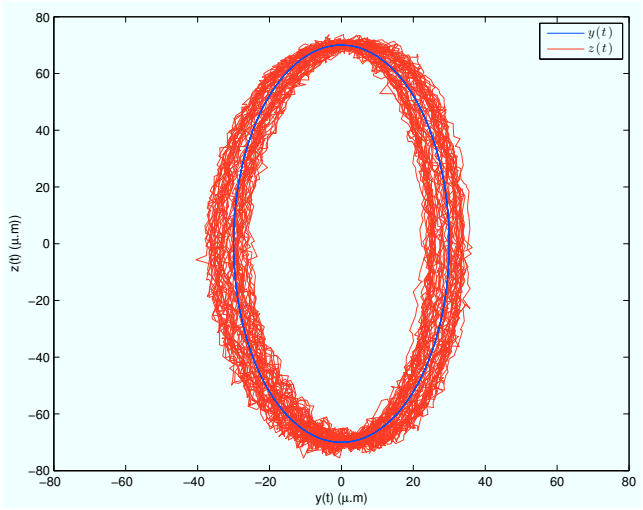

Fig. 11. Position in the $y - z$ plan before identification

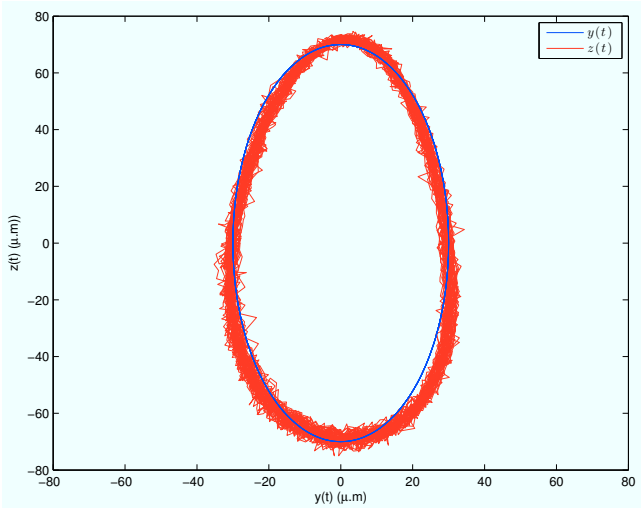

Fig. 12. Position in the $y - z$ plan after identification

[4] S. Eckhardt and J. Rudolph. High precision synchronous tool path tracking with an amb machine tool spindle, aug 3-6 2004.

[5] M. Fliess, C. Join, and M. Mboup. Algebraic change-point detection. *Applicable Algebra in Engineering, Communication and Computing*, 21:131–143, 2010.

[6] M. Fliess and H. Sira-Ramírez. An algebraic framework for linear identification. *ESAIM: COCV*, 9:151–168, jan 2003.

[7] M. Fliess and H. Sira Ramirez. Closed-loop parametric identification for continuous-time linear systems via new algebraic techniques. In H. Garnier & L. Wang, editor, *Identification of Continuous-time Models from Sampled Data*, Advances in Industrial Control, pages 362–391. Springer, 2008.

[8] A. Gensior, J. Weber, H. Guldner, and J. Rudolph. An algebraic parameter identification algorithm and asymptotic observers for estimation of the load of a boost converter. In *Industrial Electronics, 2007. ISIE 2007. IEEE International Symposium on*, pages 7 –11, 2007.

[9] T. Grochmal and A. Lynch. Control of a self-bearing servomotor. *Control Systems Magazine, IEEE*, 29(5):74–92, Oct. 2009.

[10] J. Levine, J. Lottin, and J.-C. Ponsart. A nonlinear approach to the control of magnetic bearings. *Control Systems Technology, IEEE Transactions on*, 4(5):524–544, Sep 1996.

[11] J. v. Lowis and J. Rudolph. Flatness-based trajectory tracking control of a rotationg shaft. In *Seventh International Symp. on Magnetic Bearings, Zurich*, pages 299–304, August 2000.

[12] M. Mboup, C. Join, and M. Fliess. Numerical differentiation with annihilators in noisy environment. *Numerical Algorithms*, 50:439–467, 2009. MSC : 65D25 ; 44A40 ; 44A10.

[13] J. R. Trapero, H. Sira-Ramrez, and V. Feliu Batlle. An algebraic frequency estimator for a biased and noisy sinusoidal signal. *Signal Processing*, 87(6):1188 – 1201, 2007.

[14] S. Riachy, Y. Bachalany, M. Mboup, and J.P. Richard. Différenciation numérique multivariable I : estimateurs algébriques et structure. In *Sixième Conférence Internationale Francophone d'Automatique Nancy, France, 2-4 juin 2010*, Nancy France, 2010.

[15] Z. Tiganj, M. Mboup, C. Pouzat, and B. Lotfi. An algebraic method for eye blink artifacts detection in single channel EEG recordings. In *17th International Conference on Biomagnetism BIOMAG2010*, volume 28, pages 175–178, Dubrovnik Croatie, 03 2010.

[16] J. Villagra, B. D'Andrea Novel, M. Fliess, and H. Mounier. An algebraic approach for maximum friction estimation. In *8th IFAC Symposium on Nonlinear Control Systems (NOLCOS)*, Bologna Italie, 2010. IFAC.